

ity (ischemic stroke, TIA, amaurosis fugax). RNA extracted from atherosclerotic plaques (n=78) was reverse transcribed with random primers and the resulting cDNA used as template in quantitative real time-PCR. Taqman probes were designed to selectively quantify the sIL6R. Two housekeeping genes were used to normalize gene expression. Relative difference in expression was estimated using the  $\Delta\Delta Ct$  method, where high  $\Delta Ct$  signifies low expression, and compared in patients with and without ischemic cerebrovascular events prior to endarterectomy.

**Results:** In 60-year-old subjects, free from prevalent cardiovascular disease, the risk of future ischemic stroke was increased with serum sIL6R above the median (adjusted HR 1.96; 95% CI 1.39–2.74).

In endarterectomized patients, subjects with symptomatic carotid artery stenosis (n=53) exhibited higher levels of sIL6R expression compared to those with an asymptomatic stenosis (n=25) with  $\Delta Ct$  10.51; 95% CI 10.02–11.00 vs.  $\Delta Ct$  11.05; 95% CI 10.44–11.34,  $p=0.06$ .

**Conclusions:** High serum levels of sIL6R are associated with the risk of future ischemic stroke and patients with symptomatic carotid artery stenosis have higher levels of expression of sIL6R locally in extracted carotid plaques indicating that sIL6R is a factor to account for in patients with atherothrombotic cerebrovascular events.

## P2626

### Higher dietary acids load is associated with higher likelihood of peripheral arterial disease among American adults

M. Mazidi<sup>1</sup>, D.P. Mikhailidis<sup>2</sup>, M. Banach<sup>3</sup>. <sup>1</sup>Chalmers University of Technology, Dept. of Biology and Biological Engineering, Food and Nutrition Science, Gothenburg, Sweden; <sup>2</sup>University College London, Dept. of Clinical Biochemistry, London, United Kingdom; <sup>3</sup>Medical University of Lodz, Dept. of Hypertension, Lodz, Poland. On behalf of International Lipid Expert Panel (ILEP)

**Background:** Peripheral arterial disease (PAD) increases with age, and by the age of 65 years, up to one-fifth of adults have PAD. As far as we are aware, no study examined the association between dietary acid-base load and PAD.

**Purpose:** To explore the association between dietary acid load, potential renal acid load (PRAL) and net endogenous acid production (NEAP), and peripheral arterial disease (PAD) in a national representative sample of American adults.

**Methods:** The National Health and Nutrition Examination Survey (NHANES) database (for 1999–2002) was used. PAD was diagnosed by ankle brachial index assessment. Analysis of covariance was used to examine adjusted mean of different dietary acid load by PAD status; and multivariable logistic regression used to relate dietary acid load with prevalent PAD. Sample weighting was accounted for in all analyses.

**Results:** Of the 4864 eligible participants aged 40–85, 2482 (51.0%) were men, and 269 (5.5%) had PAD. After adjustment for age-, sex-, race-, estimated glomerular filtration rate (eGFR), smoking, dietary fat, carbohydrates, protein, saturated fat, and dietary fiber, and energy intake, body mass index, hypertension, cholesterol, triglyceride and diabetes, estimated glomerular filtration rate, participants with PAD had higher mean of (PRAL: 16.2 vs 9.1 mEq/d, NEAP: 56.2 vs 50.1 mEq/d, both  $p<0.001$ ) than PAD-free participants. In logistic regression with same cofounders, the top quarter of PRAL (more acidic) was associated with 31% higher odds of the PAD compared with the bottom quarter (more alkaline) [odds ratio: 1.31, 95% confidence interval: 1.11–1.57].

**Conclusions:** Our findings, for the first time, suggest that dietary acids load, an index of acid-base balance, is associated with the likelihood of PAD after adjustment for main clinical and anthropometrical confounding factors. These results support the hypothesis that diet plays an important role in chronic disease occurrence.

## CORONARY PHYSIOLOGY AND IMAGING

## P2627

### Comparison of 3-dimensional quantitative coronary angiography and intravascular ultrasound for detecting functionally significant coronary lesions

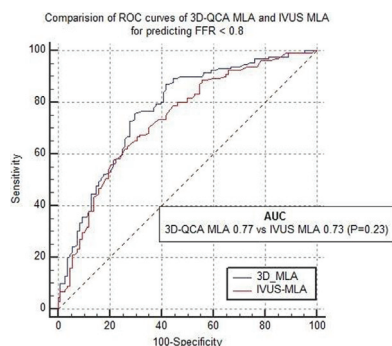
J.H. Lee, M.H. Yoon, S.J. Tahk, J.H. Shin, G.S. Hwang, S.Y. Choi, B.J. Choi, H.S. Lim, H.M. Yang, J.S. Park, K.W. Seo. *Ajou University Hospital, Cardiology, Suwon, Korea Republic of*

**Background:** Three-dimensional quantitative coronary angiography (3D-QCA) can provide more accurate measurement of true vessel size and may be comparable to intravascular ultrasound (IVUS) in identifying functionally significant coronary stenosis determined by fractional flow reserve (FFR). We aimed to evaluate diagnostic accuracy of 3D-QCA for predicting FFR  $<0.8$ .

**Methods:** We assessed 240 lesions in 213 patients by FFR, IVUS and 3D-QCA. Correlations between 3D-QCA values, IVUS values and FFR values were analyzed. The receiver operating characteristic (ROC) curves were used to evaluate diagnostic accuracy of 3D-QCA for predicting FFR  $<0.8$  and to find cut-off value.

**Results:** Of 3D-QCA values, minimum lumen area (MLA) correlated with FFR values ( $r=0.48$ ,  $p<0.001$ ). Of IVUS values, MLA correlated with FFR values ( $R=0.43$ ,  $p<0.001$ ). Also 3D-QCA MLA well correlated with IVUS MLA ( $r=0.61$ ,  $p<0.001$ ). The area under the ROC curve (AUC) for 3D-QCA MLA was 0.77 and the best cut-off value was 2.37 (sensitivity: 73%, specificity: 71%). The AUC for IVUS MLA

was 0.73 and the best cut-off value was 3.01 (sensitivity: 71%, specificity: 65%). There is no significant difference between the AUC for 3D-QCA and IVUS-QCA (AUC=0.27).



**Conclusions:** 3D-QCA is at least not inferior to IVUS for functional assessment of intermediate coronary lesions. We can consider 3D-QCA as the substitution of IVUS or FFR in deciding coronary intervention.

## P2628

### OCT-assessment of scaffold resorption: analysis of strut intensity via the brs-resorb-index for poly-L-lactic acid bioresorbable vascular scaffolds

F. Blachutzik<sup>1</sup>, S. Achenbach<sup>2</sup>, M. Troebs<sup>2</sup>, M. Marwan<sup>2</sup>, M. Weissner<sup>3</sup>, H. Nef<sup>1</sup>, C. Schlundt<sup>2</sup>. <sup>1</sup>University Hospital Giessen and Marburg, Department of Cardiology, Giessen, Germany; <sup>2</sup>University Hospital Erlangen, Department of Medicine 2 - Cardiology, Erlangen, Germany; <sup>3</sup>University Hospital Mainz, Department of Cardiology, Mainz, Germany

**Background:** Resorption of bioresorbable vascular scaffolds is influenced by numerous factors.

**Purpose:** The aim of this study was to analyze individual differences in resorption of BRS and identify factors potentially influencing the resorption process through optical coherence tomography (OCT) analysis.

**Methods:** Between April 2016 and July 2017 clinically driven invasive coronary angiography and OCT were performed in 36 patients who had previously been treated with a total of 48 BRS. OCT-analysis was performed using QCU-CMS v4.69 OCT analysis software (Leiden University Medical Center, Leiden, Netherlands). Normalized light intensity (= Number of color pixels per BRS strut divided through number of color pixels per equivalent area in the adjacent intima) of each BRS strut was calculated using ImageJ 1.51j8 (National Institutes of Health, USA). Subsequently, the BRS-RESORB-INDEX (BRI) was calculated per scaffold (=Normalized light intensity x 1000 divided through time since BRS implantation (days)).

**Results:** The mean time interval since implantation was 789±321 days (range: 380–1173). BRS struts were still discernible in all 48 BRS. Target lesion revascularization due to in-BRS restenosis was performed in 6 patients (17%) with 8 BRS (17%). Restenosis was characterized as mature neointima in all cases. Normalized light intensity as a marker for resorption of BRS struts increased with time in a linear fashion (Spearman Rho:  $p<0.001$ , correlation coefficient=0.90;  $R^2$  (linear) = 0.91). BRS resorption, as measured by the BRI, varied widely between different individuals (range: 0.09–0.85) but showed very little variability within different BRS implanted in one patient (inter-patient variance:  $0.32\pm0.38$ , intra-patient variance:  $0.02\pm0.06$ ;  $p<0.001$ ). Multivariable analysis identified diabetes (mean BRI of patients with diabetes vs. patients without diabetes:  $0.34\pm0.13$  vs.  $0.58\pm0.22$ ;  $p=0.002$ ) and presence of PSLIA (peri-strut low intensity area) (mean BRI of patients with PSLIA vs. patients without PSLIA:  $0.44\pm0.21$  vs.  $0.61\pm0.18$ ;  $p=0.027$ ) as independent predictors of prolonged BRS resorption, whereas the resorption rate in ACS patients (STEMI, NSTEMI and unstable angina; n=13) was significantly higher as compared to patients without ACS (mean BRI  $0.62\pm0.17$  vs.  $0.43\pm0.24$ ;  $p=0.012$ ).

**Conclusion:** BRS resorption rate, measured by OCT through normalized light intensity relative to time since implantation, is influenced by patient-specific characteristics. Diabetes and the presence of PSLIA are associated with a prolonged resorption process, whereas in patients after ACS, resorption appears to be significantly faster.

## P2629

### Reliability of optical coherence tomography in the prediction of occurrence of side-branch complications after percutaneous coronary intervention

S. Kimura, T. Kawakami, N. Kanehama, R. Tateishi, S. Tachibana, H. Arai, S. Hara, K. Hayasaka, J. Hiroki, K. Yoshioka, S. Kuroda, R. Iwatsuka, A. Mizukami, T. Hayashi, A. Matsumura. *Cardiology, Kamada Medical Center, Kamogawa, Japan*

**Background:** Side-branch complications after percutaneous coronary interven-

tion (PCI) may lead to poor outcomes in patients with bifurcation lesions. However, the mechanism of side-branch complications after PCI for bifurcations lesions remains unclear.

**Purpose:** We investigated the impact of lesion morphologies and plaque characteristics in coronary bifurcation lesions on the occurrence of side-branch complications.

**Methods:** We investigated 63 patients with 68 native coronary bifurcation lesions without baseline side-branch stenosis undergoing single new-generation drug-eluting stent implantation (29 bioresorbable polymer sirolimus-eluting stent (BP-SES) and 39 BP-everolimus-eluting stents (BP-EES)). All lesions underwent pre- and post-intervention optical coherence tomography (OCT). Side-branch complication was defined as side-branch stenosis (>90%) during PCI. Lesions plaque characteristics were assessed at five regions in relation to side-branch: proximal side-branch side; distal side-branch side; bifurcation site; proximal side-branch opposite side; and distal side-branch opposite side. OCT-derived longitudinal plaque distribution and morphologies, and quantitative variables related to bifurcation angles were assessed.

**Results:** Side-branch complications were observed in 31 lesions (45.6%). Lesions with side-branch complications had higher frequency of lipid-rich plaque (48.4% vs. 21.6%,  $p=0.04$ ) at bifurcation site, and lipid-rich plaque (51.6% vs. 21.6%,  $p=0.02$ ) at distal side-branch opposite side, smaller carina-tip angle ( $50.8\pm 22.5^\circ$  vs.  $78.9\pm 25.5^\circ$ ,  $p<0.001$ ), and shorter branching-point to carina-tip length ( $0.90\pm 0.26$  mm vs.  $1.44\pm 0.67$  mm,  $p<0.001$ ) than those without. Optimal cutoff value of carina-tip angle and branching-point to carina-tip length for side-branch complications was  $55.7^\circ$  (area under the curve 0.81,  $p<0.001$ ) and 1.24 mm (0.79,  $p<0.001$ ). Of 4 pre-PCI OCT features including lipid-rich plaque at bifurcation site, calcification at distal opposite side, carina-tip angle  $\leq 55.7^\circ$ , and branching-point to carina-tip length  $\leq 1.24$  mm, 3 or 4 feature positive lesions had higher prevalence of side-branch complications than 2 or less feature positive lesions (94.4% vs. 28.0%,  $p<0.001$ ). Post-PCI OCT findings showed that 54.9% of lesions with side-branch complications were related with carina-shift and 38.8% with tissue protrusion. Stent types did not influence our results.

**Conclusion:** Longitudinal plaque distribution and morphologies as well as bifurcation angles detected by OCT may influence the occurrence of side-branch complications after BP-DES.

## P2630

### Comparison of tissue characteristics in restenosis lesion between bioabsorbable polymer drug-eluting stent and durable polymer drug-eluting stent

N. Kobayashi, Y. Ito, K. Hirano, M. Yamawaki, M. Araki, T. Sakai, Y. Sakamoto, S. Mori, M. Tsutsumi, M. Nauchi, Y. Honda, K. Makino, S. Shirai. *Saiseikai Yokohama City Eastern Hospital, Yokohama, Japan*

**Background:** Polymer is considered as associating with inflammation formation and allergy and finally with late stent failure. Bioabsorbable polymer (BP) is hoped to reduce these problems compared with durable polymer (DP), however little is known about this.

**Methods:** A total of 141 in-stent restenosis (ISR) underwent optical frequency domain imaging (OFDI) or optical coherence tomography (OCT) were retrospectively identified. Of these, 88 ISR of DP drug-eluting stent (DES) and 53 ISR of BP-DES were observed.

**Results:** Restenotic tissue characteristics were compared between the groups. There was no significant difference in tissue characteristics between the groups (Homogeneous: 33% vs. 26.4%,  $P=0.414$ ; Heterogeneous: 29.5% vs. 18.3%,  $P=0.875$ ; Layered: 10.2% vs. 13.2%,  $P=0.589$ ; Neo-lipid: 22.7% vs. 24.5%,  $P=0.807$ ; Neo-calc: 6.8% vs. 9.4%,  $P=0.575$ ). In only late restenosis lesions (>1 year), restenotic tissue characteristics was also similar (Homogeneous: 27.4% vs. 29.6%,  $P=0.831$ ; Heterogeneous: 27.4% vs. 18.4%,  $P=0.371$ ; Layered: 6.5% vs. 11.1%,  $P=0.453$ ; Neo-lipid: 32.3% vs. 37%,  $P=0.661$ ; Neo-calc: 9.7% vs. 3.7%,  $P=0.336$ ).

**Conclusion:** Restenotic tissue characteristics was similar between BP-DES and DP-DES.

## P2631

### Accuracy of optical coherence tomography in predicting functional significance of coronary stenosis determined by fractional flow reserve: a meta-analysis

A. Ramasamy<sup>1</sup>, Y. Chen<sup>2</sup>, T. Zanchin<sup>3</sup>, K. Rathod<sup>1</sup>, D. Jones<sup>1</sup>, R. Parasa<sup>4</sup>, Y.J. Zhang<sup>5</sup>, R. Amersey<sup>1</sup>, M. Westwood<sup>1</sup>, M. Ozkor<sup>1</sup>, A. Baumbach<sup>1</sup>, A. Mathur<sup>1</sup>, P.W. Serruys<sup>6</sup>, T. Crake<sup>7</sup>, C.V. Bourantas<sup>1</sup>. <sup>1</sup>Barts Health NHS Trust, Department of Cardiology, London, United Kingdom; <sup>2</sup>North Middlesex University Hospital NHS Trust, University College London, London, United Kingdom; <sup>3</sup>Bern University Hospital, Department of Cardiology, Bern, Switzerland; <sup>4</sup>Princess Alexandra Hospital NHS Trust, Department of Cardiology, London, United Kingdom; <sup>5</sup>Nanjing Medical University, Nanjing First Hospital, Nanjing, China People's Republic of; <sup>6</sup>Imperial College London, International Centre for Circulatory Health, NHLI, London, United Kingdom; <sup>7</sup>University College London, Department of Cardiology, London, United Kingdom

**Background and introduction:** Fractional flow reserve (FFR) is the gold standard for physiological assessment of coronary artery disease severity and guiding

percutaneous coronary interventions. Intracoronary imaging modalities such as intravascular ultrasound (IVUS) and optical coherence tomography (OCT) can be used as adjuncts in the evaluation of coronary artery disease, providing detailed assessment of luminal dimensions, plaque composition and guide stent deployment. Several studies and meta-analyses have assessed the efficacy of IVUS compared with FFR in detecting haemodynamically significant lesions. Data for OCT is less readily available and an authoritative review of the existing evidence for OCT's efficacy in identifying functionally significant stenoses is lacking.

**Purpose:** To assess the accuracy of anatomical parameters estimated by OCT in predicting functionally significant coronary artery stenoses as determined by FFR.

**Methods:** Pubmed/Medline, Cochrane and Biomed Central were systematically searched for studies (up to February 2018) assessing the diagnostic accuracy of minimal lumen area (MLA), minimal luminal diameter (MLD) and area stenosis (AS) derived from OCT to detect coronary artery stenoses deemed functionally significant by FFR. The meta-analysis was performed following the Preferred Reporting items for reviews and meta-analyses (PRISMA).

**Results:** Out of the 385 retrieved studies, 9 studies were included in the meta-analysis enrolling 585 patients (741 lesions); 4 studies included patients with acute coronary syndrome. The mean angiographic diameter stenosis and lesion length was 48.07% and 13.65mm respectively; 7 studies used FFR <0.80 as a cut-off value for haemodynamic significance and the remaining 2 chose FFR <0.75 as the threshold.

The calculated median cut-offs for OCT parameters were MLA 1.93 mm<sup>2</sup>, MLD 1.34 mm<sup>2</sup> and AS 70%. For OCT-MLA (9 studies), the pooled area under the curve (AUC) was 0.83 (0.78–0.87) with a sensitivity of 0.76 (0.71–0.81) and specificity of 0.77 (0.73–0.82) in detecting functionally significant stenoses. OCT-MLD (7 studies) had a pooled AUC of 0.85 (0.80–0.89) with a sensitivity of 0.81 (0.74–0.86) and specificity 0.79 (0.73–0.83) and OCT-AS (4 studies) had a similar accuracy, with pooled AUC 0.80 (0.65–0.94), sensitivity 0.75 (0.66–0.83) and specificity 0.76 (0.67–0.83) in detecting functionally significant stenoses.

**Conclusions:** This meta-analysis shows that OCT has a good diagnostic accuracy in identifying functionally significant coronary artery stenoses as assessed by FFR. The efficacy of all the tested OCT parameters (MLA, MLD and AS) compares favourably to the efficacy of IVUS reported in the literature, fact that should be attributed to the superior resolution of the modality that enables more accurate evaluation of coronary artery anatomy.

## P2632

### Optical coherence tomography tissue coverage and characterization at six months after implantation of bioresorbable scaffolds versus conventional everolimus eluting stents in the ISAR-Absorb MI trial

H. Rai<sup>1</sup>, F. Alfonso<sup>2</sup>, M. Maeng<sup>3</sup>, C. Bradaric<sup>4</sup>, J. Wiebe<sup>1</sup>, J. Cuesta<sup>2</sup>, E.H. Christiansen<sup>3</sup>, J. Bohner<sup>1</sup>, P. Hoppmann<sup>1</sup>, S. Kufner<sup>1</sup>, R. Colleran<sup>1</sup>, S. Schneider<sup>4</sup>, K.L. Laugwitz<sup>4</sup>, A. Kastrati<sup>1</sup>, R.A. Byrne<sup>1</sup>. <sup>1</sup>Deutsches Herzzentrum Technische Universität, Munich, Germany; <sup>2</sup>University Hospital De La Princesa, Madrid, Spain; <sup>3</sup>Aarhus University Hospital, Aarhus, Denmark; <sup>4</sup>Hospital Rechts der Isar, Munich, Germany

**Background:** Bioresorbable scaffolds (BRS) are novel devices designed to overcome the long-term limitations of permanent metallic stent implantation. Optical coherence tomography (OCT) surveillance can provide important insights on the process of vessel wall healing at follow-up.

**Purpose:** We sought to compare OCT-assessed healing at 6 months after implantation of everolimus eluting BRS and everolimus eluting metallic stents (EES) in patients treated for acute myocardial infarction (AMI).

**Methods:** ISAR-Absorb MI is a multicentre, 2:1 randomized trial comparing outcomes of patients with AMI undergoing treatment with everolimus eluting BRS or conventional EES. Angiographic surveillance was planned for all patients at 6–8 months follow-up. Selected patients who had OCT surveillance available at follow-up were included for the present analysis. Morphometric analysis of contiguous OCT cross-sections was performed at 1 mm intervals within the stented segment at a centralized core laboratory (Qlvus 3.0.30.0). Tissue characterisation using a 256-level grey-scale signal intensity (GSI) analysis was also performed for all neointimal regions of interest (ROI) with thickness of 100 to 400  $\mu$ m (Image J software). ROI's were classified as mature using a standard cut-off GSI score of 109.7. Generalised linear mixed model (GLMM) was used as appropriate (IBM-SPSS, version 22.0).

**Results:** A total of 72 patients (83 stents) included in the BRS arm and 30 patients (36 stents) included in the EES arm was available for analysis (median interval of 218 days). Mean stented length was  $21.35\pm 8.78$  and  $21.60\pm 7.35$  mm in BRS and EES arm respectively. Minimum lumen area ( $5.35\pm 2.04$  vs.  $5.26\pm 2.00$  mm<sup>2</sup>) and minimum stent area ( $6.03\pm 1.86$  vs.  $6.21\pm 1.84$  mm<sup>2</sup>) were comparable between BRS and EES.

In total 2,221 frames (1,569 in BRS, 652 in EES) with 19,580 struts (13,022 in BRS, 6,558 in EES) were assessed. Overall strut coverage was better in the BRS group as compared to the EES group (97.5% vs. 91.4% respectively). Malapposed (1.1% vs. 0.4%) and uncovered struts (6.9% vs. 1.3%) were more common in the EES group. Mean percentage area stenosis was higher in the EES group ( $7.55\pm 11.12$  vs.  $6.16\pm 7.21\%$  respectively).

Mean neointimal thickness was higher with BRS ( $99.31\pm 35.56$  vs.  $94.13\pm 76.94$   $\mu$ m respectively,  $p=0.016$ ). GSI analysis in 89 cases (67 cases, 2,256 ROIs in BRS; 22 cases, 880 ROIs in EES) showed that mature ROIs were significantly